Dalton Transactions

Accepted Manuscript

This article can be cited before page numbers have been issued, to do this please use: S. Dey, B. S. Naidu and C. N. R. Rao, *Dalton Trans.*, 2016, DOI: 10.1039/C5DT04822B.

ROYAL SOCIETY OF CHEMISTRY

www.rsc.org/dalton

ROYAL SOCIETY OF CHEMISTRY View Article Online
DOI: 10.1039/C5DT04822B

Journal Name

COMMUNICATION

Beneficial effects of substituting trivalent ions in the B-site of $La_{0.5}Sr_{0.5}Mn_{1-x}A_xO_3$ (A=Al, Ga, Sc) on the thermochemical generation of CO and H_2 from CO_2 and H_2O

Received 00th January 20xx,
Accepted 00th January 20xx

DOI: 10.1039/x0xx00000x

www.rsc.org/

Sunita Dey,[a] B. S. Naidu[a] and C. N. R. Rao[a,*]

The effect of substitution of Al^{3+}, Ga^{3+} and Sc^{3+} ions in the Mn^{3+} site of $La_{0.5}Sr_{0.5}MnO_3$ on the thermochemical splitting of CO_2 to generate CO has been studied in detail. Both $La_{0.5}Sr_{0.5}Mn_{1-x}Ga_xO_3$ and $La_{0.5}Sr_{0.5}Mn_{1-x}Sc_xO_3$ give high yields of O_2 and generate CO more efficiently than $La_{0.5}Sr_{0.5}Mn_{1-x}Al_xO_3$ or the parent $La_{0.5}Sr_{0.5}MnO_3$. Substitution of even 5% Sc^{3+} (x=0.5) results in a remarkable improvement on performance. Thus $La_{0.5}Sr_{0.5}Mn_{0.95}Sc_{0.05}O_3$ produces 417 µmol/g of O_2 and 545 µmol/g of CO respectively, i.e. 2 and 1.7 times more O_2 and CO than $La_{0.5}Sr_{0.5}MnO_3$. This manganite also generates H_2 satisfactorily by the thermochemical splitting of H_2O.

Solar-thermochemical splitting of H_2O and CO_2 to generate H_2 and CO has excellent scope for improving solar- to-fuel conversion efficiency and is a potential alternative to satisfy the present day energy and environmental needs.[1-3] Thermochemical splitting of CO_2 and H_2O involving a two-step process using metal oxides (MO_n) is of special interest in this context. The basic reactions are as follows,

$$\text{Endothermal Step: } MO_n \rightarrow MO_{n-\delta} + \delta/2\, O_2 \quad ------(1)$$

$$\text{Exothermal step: } MO_{n-\delta} + \delta CO_2 \rightarrow MO_n + \delta CO$$

$$MO_{n-\delta} + \delta H_2O \rightarrow MO_n + \delta H_2 \quad ----(2)$$

Ideally, oxides which lose oxygen on heating (reduction, step 1) and reoxidize reversibly on interaction with H_2O or CO_2 (oxidation, step 2) can best serve the purpose. Nonstoichiometric oxides such as ferrites, [4-6] CeO_2 [7, 8] and doped CeO_2 [9-11] have been examined for the purpose. Doping CeO_2 with isovalent $Zr^{4+}$and Hf^{4+} has given some promising results in fuel production.[10-13] Perovskite oxides, $La_{1-x}Sr_xMnO_3$ (LSM) involving Mn^{3+}/ Mn^{4+} redox active ions have recently emerged to be superior candidates to split CO_2 and H_2O.[14] Further improvement has been achieved with $La_{1-x}Ca_xMnO_3$ perovskites.[15] Decreasing the size of the lanthanides improves the fuel production substantially, with the highest CO production obtained with $Y_{0.5}Sr_{0.5}MnO_3$.[16] B-site substituted perovskites involving combinations of Mn, Co, Fe, Cr, Al, Mg have yielded some encouraging results.[17-26] Remarkable improvement in the production of H_2 (CO) by Sr- and Al- doped $LaMnO_3$ in comparison with CeO_2 has been reported by McDaniel et al.[17] Aluminium doping appears to enhance fuel production of $La_{1-x}Sr_xMnO_3$ significantly.[27 28] Deml et al. [29] have presented a material design strategy for two-step cycles based on DFT calculations as well as experimental results on the $La_{1-x}Sr_xMn_{1-y}Al_yO_3$ perovskites. $LaGaO_3$ is known as an ionic conductor and introduction of transition metal ions in its lattice results in mixed ionic electronic conductors leading to as solid oxide fuel cell (SOFC) electrodes.[30, 31] Ga^{3+} doping in La-Sr-Fe based perovskites increases the oxygen nonstoichiometry[32-34] while Sc^{3+} increases the oxygen ion mobility in LSM perovskites and can be employed for the oxygen reduction reaction and in SOFC cathode.[32, 35-37] Considering the properties of derivatives of $LaGaO_3$ and of Sc^{3+} substituted of LSM perovskites, Ga^{3+} and Sc^{3+} substituted oxide perovskites would be expected to be good candidates for the thermochemical generation of CO and H_2. We have investigated the effect of substitution of Ga^{3+} and Sc^{3+} in the B site of $La_{0.5}Sr_{0.5}MnO_3$ (LSM50) in comparison with the effect of Al^{3+} substitution.[17,27] We have observed highly improved performance of Ga^{3+} and Sc^{3+} substituted LSMs, with the Sc^{3+} derivative giving remarkable fuel yield.

$La_{0.5}Sr_{0.5}MnO_3$ (LSM50) substituted with different proportions of Al^{3+}, Ga^{3+} and Sc^{3+}. $La_{0.5}Sr_{0.5}Mn_{1-x}A_xO_3$ (A=Al, Ga and Sc) were prepared by the sol-gel method starting with metal nitrates. The gels were heated upto 1400°C to obtain the oxides with particle sizes in the micrometer regime (details of synthesis condition and characterization techniques are in ESI, section S-A and Table S1). We have prepared the Al^{3+} substituted LSMs upto x=0.5, while in the case of Ga^{3+} and Sc^{3+}, the compositions were limited upto x=0.35 (secondary phases precipitates for

[a] Chemistry and Physics of Materials Unit, New Chemistry Unit, Sheikh Saqr Laboratory, International Centre for Materials Science (ICMS), and CSIR Centre of Excellence in Chemistry. Jawaharlal Nehru Centre for Advanced Scientific Research (JNCASR). Jakkur P.O., Bangalore- 560 064, India
* E-mail: cnrrao@jncasr.ac.in

Electronic Supplementary Information (ESI) available: [synthesis conditions, experimental details, pxrd and tga plots and tables]. See DOI: 10.1039/x0xx00000x

View Article Online
DOI: 10.1039/C5DT04822B

x>0.35) and x=0.1 (Sc_2O_3 segregates [37] for x>0.1) respectively (Fig. S1 and Fig. S2). All the perovskite oxides crystallize in the R-3c space group, as observed by the PXRD patterns in Figs. S3-S5 (Table S2, ESI). The tolerance factor of the perovskite increases with x in the Al^{3+} and Ga^{3+} derivatives but decreases with x in the case of Sc^{3+} derivatives, as the size of Sc^{3+} is larger than Mn^{3+} (Table S2, Eqn. S6 in section S-C, ESI). FESEM images and energy dispersive X-ray (EDX) mapping reveal that the as-synthesized oxides comprise of micron-sized particles and confirms the homogenous distribution of metal cations as shown in Figs. S6 and S7. The BET surface area is of around 1-2 m^2/g. Reduction of the oxide and splitting of CO_2 accompanied by the formation of CO was studied by thermogravimetric analysis (TGA). Splitting of H_2O was studied by using a locally fabricated set-up incorporating a gas chromatograph-TCD (see section S-A-3, ESI).[15] The reduction and oxidation temperatures in CO_2 (or H_2O) splitting studies were 1400°C and 1100°C respectively.

In Fig. 1, we show representative TGA curves of $La_{0.5}Sr_{0.5}Mn_{1-x}Al_xO_3$ along with the histogram of thermochemical splitting of CO_2 for x=0.25-0.5. The amount of O_2 and CO produced increases with Al^{3+} content giving the highest values of O_2 and CO produced when x=0.5. Thus, the quantities of O_2 and CO produced by the x=0.5 composition are 322 and 388 µmol/g respectively. $La_{0.5}Sr_{0.5}Mn_{0.5}Al_{0.5}O_3$ was also subjected to multiple cycling (Fig. S8) in the temperature range of 1400-1100°C, and 370 µmol/g of CO on average was obtained during three successive cycles without significant deviation in activity. The structures and compositions of the oxides remained the same after multiple cycling (Fig. S9, Table S3).

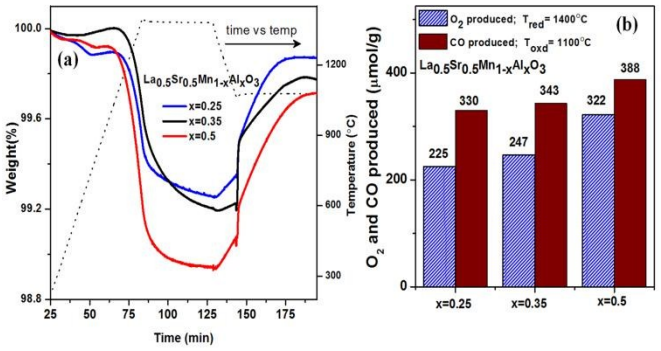

Fig. 1. (a) Representative TGA and (b) corresponding histogram of thermochemical CO_2 splitting of $La_{0.5}Sr_{0.5}Mn_{1-x}Al_xO_3$ (x= 0.25, 0.35 and 0.5). Reduction and oxidation temperatures are 1400 °C and 1100°C respectively.

$La_{0.5}Sr_{0.5}Mn_{1-x}Ga_xO_3$ behaves somewhat similar to the Al^{3+} substituted perovskites. The amount of O_2 evolved increases with x (Fig. 2). For, x=0.35, O_2 evolved 323 µmol/g (δ=0.2; % X_{red}=57), higher than x=0.25 (δ=0.18; % X_{red}=54) (Fig. S10; Eqn. S1-S5 in section S-B, ESI). In earlier reports, doping of Ga^{3+} in the B site of La-Sr-Fe perovskite has been reported to decrease the Fe-O bond covalency and increase in oxygen nonstoichiometry. [32-34, 38, 39] Ga^{3+} substitution is reported to decrease the enthalpy and increase the entropy of oxygen vacancy formation in $La_{0.3}Sr_{0.7}FeO_3$ and also induce local lattice inhomogeneties.[33]

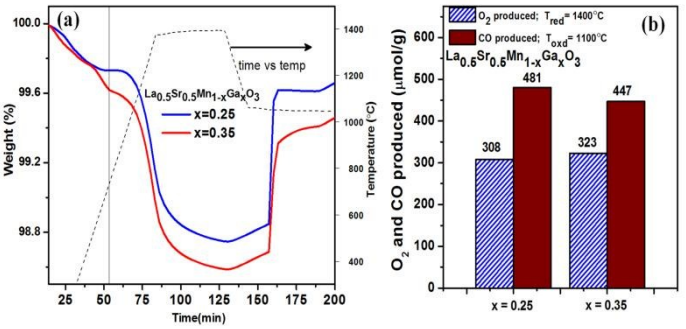

Fig. 2. (a) Representative TGA and (b) corresponding histogram of thermochemical CO_2 splitting of $La_{0.5}Sr_{0.5}Mn_{1-x}Ga_xO_3$ (x= 0.25, 0.35). Reduction and oxidation temperatures are 1400 °C and 1100°C respectively.

We have investigated the thermochemical splitting of CO_2 by $La_{0.5}Sr_{0.5}Mn_{1-x}Ga_xO_3$ (x=0.25, 0.35) by injecting CO_2 (Fig. 2) at 1100°C. Ga^{3+} substituted perovskites yield a much higher quantity of CO (447 µmol/g) even for x=0.35 as shown in Fig. 2. The quantity of CO obtained with x=0.25 is higher (480 µmol/g). The reoxidation yield (%α) of x=0.25 is 42%, higher than x=0.35 (40%) (Fig. S10).

We could substitute Sc^{3+} in the B site of LSM only upto x=0.1 (Fig. S2).[37] However, even with x=0.05, the yield of O_2 and subsequently CO are both high, the values being 417 µmol/g (δ=0.21; % X_{red}=72) and 545 µmol/g respectively (Figs. 3 and S11). Increasing the Sc^{3+} content to x=0.1 does not improve O_2 production (426 µmol/g, δ=0.21; % X_{red}=73%) as well as CO production (491 µmol/g). The reoxidation yields are 65% and 58% respectively for x=0.05 and x=0.1 in the Sc^{3+} derivatives (Fig. S11).

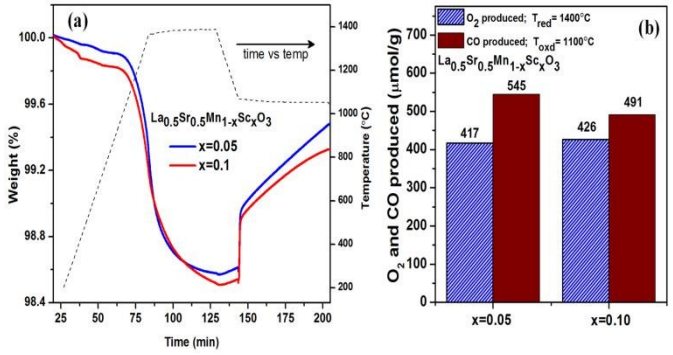

Fig. 3. (a) Representative TGA and (b) corresponding histogram of thermochemical CO_2 splitting of (a) $La_{0.5}Sr_{0.5}Mn_{1-x}Sc_xO_3$ (x= 0.05, 0.1). Reduction and oxidation temperatures are 1400 °C and 1100°C respectively.

Sc^{3+} doping (5-10%) is reported to enhance the performance of $La_{0.8}Sr_{0.2}MnO_3$ (LSM20) as a SOFC cathode and in methane oxidation. [35, 37] This is because of the higher oxygen vacancy ratio and enhanced oxygen mobility related to the bigger size of Sc^{3+}. [35-37, 40, 41] Over doping of Sc^{3+} (>10%) in LSM20 acts as an anion vacancy trapping centre through the association of Sc^{3+} with oxygen vacancy and is reported to deteriorate the oxygen conductivity in SOFC cathodes. This may be the reason why no further increment in O_2 evolution occurs beyond x=0.05.[36, 37]

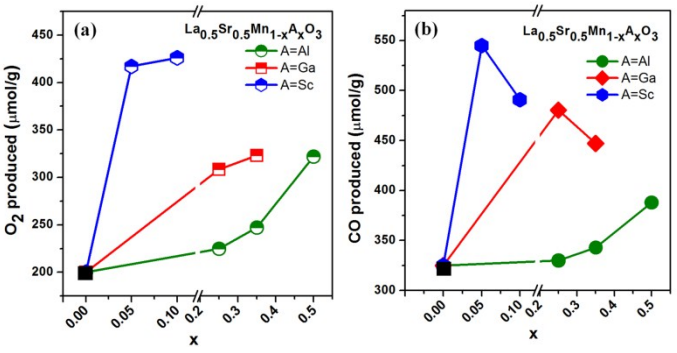

Fig. 4. Comparative study of (a) O_2 (T_{red}=1400°C) and (b) CO (T_{oxd}=1100°C) evolution with amount of Mn site substituent of $La_{0.5}Sr_{0.5}Mn_{1-x}A_xO_3$ perovskites (A=Al, Ga, Sc; 100x= % of substituent)

In Fig. 4 we compare the relative performance of the Al^{3+}, Ga^{3+} and Sc^{3+} substituted LSMs. All these derivatives show better performance than the parent LSM. Clearly the effect of the valent ions varies as Sc>Ga>Al. For the same proportions of the trivalent ion (25%), yield of O_2 is 1.4 times higher in the Ga derivative compared to the Al derivative. Increase in O_2 yield is more remarkable in Sc derivative where the x=0.05 composition produces 1.9 times and 1.3 times O_2 compared to the x=0.25 and x=0.5 composite with Al (Fig. 4a). CO yield of Ga derivative is of 1.5 times higher than Al derivative for similar proportions of x=0.25 (Fig. 4b). The increase in CO yield due to 5% Sc substitution is 1.7 times and 1.4 times of x=0.25 and x=0.5 composite with Al respectively (Fig. 4b). Notably, the CO production of x=0.25 Ga substitution and x=0.05 Sc substitution is of 1.5 times and 1.7 times of parent LSMs respectively.

We have examined the fuel production by the Ga (25%) and Sc (5%) substituted LSMs over three cycles in the 1400˚C-1100˚C temperature range (Figs. S12 and S13). The yields of O_2 and CO are affected marginally, the decrease after the third cycle less than 15-20%. The amount of CO produced by $La_{0.5}Sr_{0.5}Mn_{0.75}Ga_{0.25}O_3$ during the 1st, 2nd and 3rd cycles are 515, 437 and 429 µmol/g respectively while the CO produced by $La_{0.5}Sr_{0.5}Mn_{0.95}Sc_{0.05}O_3$ during the 1st, 2nd and 3rd cycles are 547, 496 and 476 µmol/g respectively. Decrease in fuel yield during multiple cycling is observed for most of the perovskites due to the sluggish kinetics or sintering.[17, 18, 23] Nonetheless, the CO produced in both Ga (25%) and Sc (5%) substituted perovskites even after the third cycle is higher than that found with parent LSM (316 µmol/g) or with x=0.5 substitution of Al (366 µmol/g). The structures and compositions of perovskites remain unaltered after TGA cycling as observed in PXRD (Fig. S14) and EDS analysis (Figs. S15-S16, Tables S4 and S5) although sintering of the particles is revealed by FESEM images (Fig. S15).

The increase in the weight of the nonstoichiometric oxide on passing CO_2 could partly arise from carbonate formation instead of oxidation alone. [42] Substitution of Al in LSM lattice has shown to diminish the carbonate formation by Galvez et al.[42] However, the carbonates are decomposes well below 1000˚C, while the CO_2 decomposition temperature is 1100˚C in all our experiments. We also ensured no further gain in weight occurs at high temperature due to carbonate formation as well by performing separate TG experiments on Ga and Sc substituted perovskites (experimental details at section S-A-3(ii), ESI).[42] $La_{0.5}Sr_{0.5}Mn_{0.75}Ga_{0.25}O_3$ shows no weight loss corresponding to low temp decomposition (~940°C) of carbonate, while expose to CO_2 (Fig. S17a). No extra weight gain is obtained during the oxidation under 850°C in compare to regular oxidation of 1100°C (Fig. S17b), further reconfirms the weight gain is due to the CO_2 splitting. Similar conclusion has been obtained with $La_{0.5}Sr_{0.5}Mn_{0.95}Sc_{0.05}O_3$ (Fig. S18). The slow rate of oxidation can be due to kinetic barriers, as the oxidation is performed at a significantly lower temperature (700°C/850°C). The onset of mass loss remains the same during reduction under Ar as shown by the vertical lines in Figs. S17b and S18b. Interestingly, few earlier reports suggested that Sc^{3+} doping on LSMs suppress the SrO segregation, which actually promotes carbonate formation by CO_2 adsorption.[35, 36] It further strengthens our observation and highlighted the advantages of $Sc^{3+}$and Ga^{3+} doping.

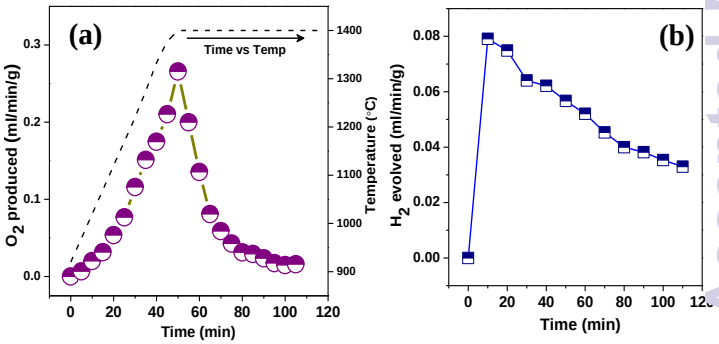

Fig. 5. (a) O_2 and (b) H_2 evolution profile of $La_{0.5}Sr_{0.5}Mn_{0.95}Sc_{0.05}O_3$. Reduction and H_2O splitting temperatures are 1400 °C and 1100°C respectively.

$La_{0.5}Sr_{0.5}Mn_{0.95}Sc_{0.05}O_3$ gave superior performance with high CO productivity even during multiple cycling; we have employed it for water splitting (see section S-A-3(iii), ESI). Production of O_2 and H_2 was detected by gas chromatograph, shown in Fig. 5. The O_2 production starts at 900°C and completes within 40 mins after reaching 1400°C. The total amount of O_2 produced is 390 µmol/g, close to the yield during TG measurements. H_2 is detected immediately after the entrance of H_2O in the gas stream (T_{oxd}=1100˚C), and the quantities reaches a maximum and decreases thereafter (Fig. 5b). The amount of H_2 produced in a span of 100 mins is approximately 250 µmol/g. H_2 evolution has not been completed even after 100 mins. The kinetic behaviour of H_2O splitting of $La_{0.5}Sr_{0.5}Mn_{0.95}Sc_{0.05}O_3$ is comparable to that of CO_2 splitting (Fig. S19 and Table S6). H_2 is produced in the initial 100mins of the reaction in the fast kinetic regime (yellow region, step 1, Fig. S19), followed by a slower kinetic regime (grey region, step 2, Fig. S19).

Conclusions

In conclusion, Ga and Sc substituted LSM based perovskites have been exploited for the first time for thermochemical CO_2 and H_2O splitting and these oxides show superior performance

in comparison with Al substituted LSMs or the parent LSM. It is noteworthy that the oxidation state of Ga and Sc remain +3 throughout and the effect of the trivalent cations varies in the order, Sc>Ga>Al. For the same proportion of the trivalent ion (25%), the yields of O_2 and CO are 1.4 and 1.5 times higher in the Ga derivative compared to the Al derivative. The performance obtained with substitution of 5% Sc^{3+} ($La_{0.5}Sr_{0.5}Mn_{0.95}Sc_{0.05}O_3$) is remarkable with O_2 and CO yields of almost 2 and 1.7 times more than the parent LSM. Carbonate formation has not observed to contribute in weight gain during oxidation. Furthermore, 250 µmol/g of H_2 is produced with $La_{0.5}Sr_{0.5}Mn_{0.95}Sc_{0.05}O_3$ at 1100˚C. Incorporation of Ga^{3+} and Sc^{3+} in the LSM50 perovskite is beneficial in the two-step fuel production process and can be employed for high temperature syngas production and other applications.

Acknowledgements

SD thanks CSIR for fellowship.

References

1 T. Kodama and N. Gokon, *Chem. Rev.*, 2007, **107**, 4048-4077.
2 J. E. Miller, A. Ambrosini, E. N. Coker, M. D. Allendorf and A. H. McDaniel, *Energy Procedia*, 2014, **49**, 2019-2026.
3 M. Roeb, M. Neises, N. Monnerie, F. Call, H. Simon, C. Sattler, M. Schmucker and R. Pitz-Paal, *Materials*, 2012, **5**, 2015-2054.
4 Y. Tamaura, A. Steinfeld, P. Kuhn and K. Ehrensberger, *Energy*, 1995, **20**, 325-330.
5 F. He and F. Li, *Energy Environ. Sci.*, 2015, **8**, 535-539.
6 C. L. Muhich, B. D. Ehrhart, V. A. Witte, S. L. Miller, E. N. Coker, C. B. Musgrave and A. W. Weimer, *Energy Environ. Sci.*, 2015, **8**, 3687-3699.
7 S. Abanades and G. Flamant, *Sol. Energy*, 2006, **80**, 1611-1623.
8 W. C. Chueh, C. Falter, M. Abbott, D. Scipio, P. Furler, S. M. Haile and A. Steinfeld, *Science*, 2010, **330**, 1797-1801.
9 A. Le Gal and S. Abanades, *J. Phys. Chem. C*, 2012, **116**, 13516-13523.
10 J. R. Scheffe, R. Jacot, G. R. Patzke and A. Steinfeld, *J. Phys. Chem. C* 2013, **117**, 24104-24114.
11 Y. Hao, C.-K. Yang and S. M. Haile, *Chem. Mater.*, 2014, **26**, 6073-6082.
12 M. Kang, J. Zhang, C. Wang, F. Wang, N. Zhao, F. Xiao, W. Wei and Y. Sun, *RSC Adv.*, 2013, **3**, 18878-18885.
13 E. V. Ramos-Fernandez, N. R. Shiju and G. Rothenberg, *RSC Adv.*, 2014, **4**, 16456-16463.
14 J. R. Scheffe, D. Weibel and A. Steinfeld, *Energy Fuels*, 2013, **27**, 4250-4257.
15 S. Dey, B. S. Naidu, A. Govindaraj and C. N. R. Rao, *Phys. Chem. Chem. Phys.*, 2015, **17**, 122-125.
16 S. Dey, B. S. Naidu and C. N. R. Rao, *Chem. Eur. J.*, 2015, **21**, 7077-7081.
17 A. H. McDaniel, E. C. Miller, D. Arifin, A. Ambrosini, E. N. Coker, R. O'Hayre, W. C. Chueh and J. Tong, *Energy Environ. Sci.*, 2013, **6**, 2424-2428.
18 A. Demont and S. Abanades, *J. Mater. Chem. A*, 2015, **3**, 3536-3546.
19 A. Demont and S. Abanades, *RSC Adv.*, 2014, **4**, 54885-54891.
20 A. H. Bork, M. Kubicek, M. Struzik and J. L. M. Rupp, *J. Mater. Chem. A*, 2015, **3**, 15546-15557.
21 C.-K. Yang, Y. Yamazaki, A. Aydin and S. M. Haile, *J. Mater. Chem. A*, 2014, **2**, 13612-13623.
22 Q. Jiang, J. Tong, G. Zhou, Z. Jiang, Z. Li and C. Li, *Sol. Energy*, 2014, **103**, 425-437.
23 A. Demont, S. Abanades and E. Beche, *J. Phys. Chem. C*, 2014, **118**, 12682-12692.
24 L. Nalbandian, A. Evdou and V. Zaspalis, *Int. J. Hydrogen Energy*, 2009, **34**, 7162-7172.
25 A. A. Leontiou, A. K. Ladavos, A. E. Giannakas, T. V. Bakas and P. J. Pomonis, *J. Catal.*, 2007, **251**, 103-112.
26 A. A. Leontiou, A. K. Ladavos, T. V. Bakas, T. C. Vaimakis and P. J. Pomonis, *Appl. Catal. A: Gen.*, 2003, **241**, 143-154.
27 T. Cooper, J. R. Scheffe, M. E. Galvez, R. Jacot, G. Patzke and A. Steinfeld, *Energy Technology*, 2015, **3**, 1130-1142.
28 M. Takacs, M. Hoes, M. Caduff, T. Cooper, J. R. Scheffe and A. Steinfeld, *Acta Materialia*, 2016, **103**, 700-710.
29 A. M. Deml, V. Stevanovic, A. M. Holder, M. Sanders, R. O'Hayre and C. B. Musgrave, *Chem. Mater.*, 2014, **26**, 6595-6602.
30 S. J. Skinner and J. A. Kilner, *Materials Today*, 2003, **6**, 30-37.
31 F. Chen and M. Liu, *J. Solid State Electrochem.*, 1998, **3**, 7-14.
32 V. V. Kharton, M. V. Patrakeev, J. C. Waerenborgh, V. A. Sobyanin, S. A. Veniaminov, A. A. Yaremchenko, P. Gaczynski, V. D. Belyaev, G. L. Semin and J. R. Frade, *Solid State Sciences*, 2005, **7**, 1344-1352.
33 M. V. Patrakeev, E. B. Mitberg, A. A. Lakhtin, I. A. Leonidov, V. L. Kozhevnikov, V. V. Kharton, M. Avdeev and F. M. B. Marques, *J. Solid State Chem,*, 2002, **167**, 203-213.
34 E. N. Naumovich, M. V. Patrakeev, V. V. Kharton, M. S. Islam, A. A. Yaremchenko, J. R. Frade and F. M. B. Marques, *Solid State Ionics*, 2006, **177**, 457-470.
35 C. Zhang, Y. Zheng, Y. Lin, R. Ran, Z. Shao and D. Farrusseng, *J. Power Sources*, 2009, **191**, 225-232.
36 H. Gu, Y. Zheng, R. Ran, Z. Shao, W. Jin, N. Xu and J. Ahn, *J. Power Sources*, 2008, **183**, 471-478.
37 X. Yue, A. Yan, M. Zhang, L. Liu, Y. Dong and M. Cheng, *J. Power Sources*, 2008, **185**, 691-697.
38 V. V. Kharton, E. V. Tsipis, A. A. Yaremchenko, I. P. Marozau, A. P. Viskup, J. R. Frade and E. N. Naumovich, *Materials Science and Engineering: B*, 2006, **134**, 80-88.
39 M. V. Patrakeev, V. V. Kharton, Y. A. Bakhteeva, A. L. Shaula, I. A. Leonidov, V. L. Kozhevnikov, E. N. Naumovich, A. A. Yaremchenko and F. M. B. Marques, *Solid State Sciences*, 2006, **8**, 476-487.
40 D. Lybye, F. W. Poulsen and M. Mogensen, *Solid State Ionics*, 2000, **128**, 91-103.
41 H. Ullmann and N. Trofimenko, *Solid State Ionics*, 1999, **119**, 1-8.
42 M. E. Galvez, R. Jacot, J. Scheffe, T. Cooper, G. Patzke and A. Steinfeld, *Phys. Chem. Chem. Phys.*, 2015, **17**, 6629-6634.